Available online at www.sciencedirect.com

SCIENCE DIRECT®

Polyhedron 24 (2005) 2437–2442

POLYHEDRON

www.elsevier.com/locate/poly

Synthesis, structure and magnetic properties of pyrazolate-bridged dinuclear complexes $[\{M(NCS)(4\text{-Phpy})\}_2(\mu\text{-bpypz})_2]$ ($M = Co^{2+}$ and Fe^{2+})

Ko Yoneda, Keisaku Nakano, Junji Fujioka, Koichi Yamada, Takayoshi Suzuki, Akira Fuyuhiro, Satoshi Kawata, Sumio Kaizaki *

Department of Chemistry, Graduate School of Science, Osaka University, Toyonaka, Osaka 560-0043, Japan

Received 5 October 2004; accepted 31 October 2004
Available online 19 May 2005

Abstract

The synthesis and magnetic characterization of pyrazolato-bridged dinuclear complexes $[\{M(NCS)(4\text{-Phpy})\}_2(\mu\text{-bpypz})_2]$ (Hbpypz = 3,5-bis(2-pyridyl)-pyrazole; 4-Phpy = 4-phenylpyridine; $M = Co^{2+}$ (**1**) and Fe^{2+} (**2**)) are described together with the X-ray crystal analysis of the cobalt complex. The structure of **1** shows that the desired coordination has been achieved with the cobalt atoms being coordinated to two bpypz to form the dimer. The X-ray diffraction patterns show **1** and **2** to be isomorphous at room temperature. **2** displays a single spin-crossover transition between the [HS–HS] and [LS–LS] states with $T_c = 150$ K.

Keywords: Dinuclear complex; Spin-crossover; 3,5-Bis(2-pyridyl)-pyrazole; 4-Phenylpyridine

1. Introduction

The spin-crossover between low-spin and high-spin states is a type of molecular magnetism that occurs in some six-coordinate, first row transition metal complexes [1,2]. This phenomenon is one of the most spectacular examples of molecular bistability driven by external constraints leading to molecular switch or memory [3,4]. The fundamental origin of the spin-crossover phenomenon is molecular, but the magnetic behavior strongly depends on intermolecular interaction. Up to now, the major source of information on spin transition systems comes from mononuclear iron(II) compounds where molecular distortions spread through the whole crystal by means of intermolecular interactions. However, the cooperativity in the systems would be enhanced by controlling both intra- and intermolecular interactions if polynuclear compounds are employed [5–8]. Thus, the cooperativity can be achieved by using suitable bridging ligands. A series of dimeric and polymeric iron(II) spin-crossover compounds were synthesized and magnetically characterized along this line while the crystal structures were not determined. Real et al. [9–14] investigated the LIESST effect on the dinuclear iron(II) compounds and pointed out a form of synergy between magnetic interaction and spin conversion in the presence of light. However, there are no X-ray analysis for dinuclear complexes until the first X-ray structure of the spin-crossover dinuclear diiron(II) complex was very recently reported for $[\{Fe(NCSe)(\mu\text{-pzpy})(pzpyH)\}_2]$ (pzpyH = 2-pyrazolylpyridine) by Murray and co-workers [15]. Shortly later, we studied the X-ray structure of $[\{Fe(NCBH_3)(py)\}_2(\mu\text{-bpypz})_2]$ (Hbpypz = 3,5-bis(2-pyridyl)-pyrazole) and the magnetic properties of $[\{Fe(NCX)(py)\}_2(\mu\text{-bpypz})_2]$ (X = S,

---

* Corresponding author. Tel.: +81668505409; fax: +81668505408.
E-mail address: kaizaki@chem.sci.osaka-u.ac.jp (S. Kaizaki).

0277-5387/$ - see front matter
doi:10.1016/j.poly.2005.03.047

BH_3) [16,17]. We found the changes of the spin-crossover temperature T_c with S/BH_3 substitution depends on the enthalpy, presumably arising from the ligand-field strength. To get the further insight into the cooperativity between dinuclear complexes and the synergy between the intra-dimer magnetic exchange coupling and the spin-crossover phenomenon, we report here the synthesis and magnetic characterization of $[\{M(NCS)(4\text{-Phpy})\}_2(\mu\text{-bpypz})_2]$ ($M = Co^{2+}$ and Fe^{2+}). As the additional axial pyridine derivatives and the metal ions are replaceable for the bpypz-bridged dinuclear complexes, the role of these items on the spin-crossover is investigated.

2. Experimental

2.1. Syntheses

2.1.1. Preparation of the starting complexes

The starting complex *trans*-$[Fe(NCS)_2(py)_4]$ was obtained by a method given in the literature [18]. *trans*-$[Co(NCS)_2(py)_4]$ was obtained by the analogous method to *trans*-$[Fe(NCS)_2(py)_4]$; to an aqueous solution (250 mL) containing 14.58 g of $Co(NO_3)_2 \cdot 6H_2O$ and pyridine (20 mL) was slowly added an aqueous solution (100 mL) containing 8.04 g of NaNCS. The pink precipitate obtained was filtered off and washed with 10 mL portions of ethanol–pyridine (9:1). After drying in vacuo, a pink powder was obtained.

2.1.2. $[\{Co(NCS)(4\text{-Phpy})\}_2(\mu\text{-bpypz})_2]$

A methanolic solution (2 mL) of *trans*-$[Co(NCS)_2(py)_4]$ (3 $mmol\,L^{-1}$) was transferred to a glass tube, and then a methanolic solution of 2 mL of Hbpypz (3 $mmol\,L^{-1}$) and 4-Phpy (10 $mmol\,L^{-1}$) was poured into the glass tube without mixing the solutions. Orange crystals began to form at ambient temperature in 2 weeks. One of these crystals was used for X-ray crystallography. Physical measurements were conducted on a polycrystalline powder that was synthesized as follows: Hbpypz (0.022 g, 0.099 mmol) was dissolved in 12 mL of a methanol solution of 4-Phpy (0.022 g, 0.14 mmol) with a 10% methanol solution of tetra-*n*-butylammonium hydroxide $(n\text{-Bu})_4NOH$ (0.26 g, 0.10 mmol). To this solution was added 15 mL of a methanol solution of *trans*-$[Co(NCS)_2(py)_4]$ (0.049 g, 0.10 mmol) under an N_2 stream. An orange precipitate was obtained and after stirring this reaction mixture for 2 h, the precipitate was filtered off and washed with methanol. The solid was then dried in vacuo. Yield 71%. Calc. for $C_{50}H_{36}N_{12}S_2Co_2$: C, 60.85; H, 3.68; N, 17.04. Found: C, 59.61; H, 3.48; N, 17.54%. The homogeneity of the powder sample was confirmed by comparison of the observed powder diffraction pattern with that calculated from the single-crystal data.

2.1.3. $[\{Fe(NCS)(4\text{-Phpy})\}_2(\mu\text{-bpypz})_2]$

Hbpypz (0.074 g, 0.033 mmol) was dissolved in 36 mL of a methanol solution of 4-Phpy after deprotonating with a 10% methanol solution of tetra-*n*-butylammonium hydroxide $(n\text{-Bu})_4NOH$ (0.87 g, 0.34 mmol). To this solution was added 15 mL of a methanol solution of *trans*-$[Fe(NCS)_2(py)_4]$ (0.16 g, 0.33 mmol) under an N_2 stream. A yellow precipitate was obtained and after stirring this reaction mixture for 2 h, the precipitate was filtered off and washed with methanol. The solid was then dried in vacuo. Yield 71%. Calc. for $C_{50}H_{36}N_{12}S_2Fe_2$: C, 61.23; H, 3.70; N, 17.14. Found: C, 60.10; H, 3.52; N, 16.72%.

2.2. Physical measurements

Magnetic susceptibility data were recorded over the temperature range from 2 to 300 K in the presence of a magnetic field between 50 and 5000 G with a SQUID susceptometer (Quantum Design, San Diego, CA). All data were corrected for diamagnetism, which was calculated from Pascal's tables. Least squares fitting of the magnetic susceptibility to appropriate equations with Heisenberg Hamiltonian ($H = -JS_i \cdot S_j$) were performed for the cobalt complex. X-ray powder diffraction data were collected on a Rigaku MultiFlex diffractometer by using Cu Kα radiation.

2.3. Crystallographic data collection and refinement of the structure

Data collection of **1** was carried out by a Rigaku Mercury charge coupled device (CCD) system with graphite-monochromated Mo Kα radiation. Crystallographic data are given in Table 1. The structure was solved by a standard direct method (TEXSAN crystallographic software package of the Molecular Structure

Table 1
Crystallographic data for **1**

Formula	$C_{50}H_{36}Co_2N_{12}S_2$
Molecular weight	986.90
Crystal system	triclinic
Space group	$P\bar{1}$ (No. 2)
Z	1
T (K)	200
a (Å)	9.271(4)
b (Å)	10.657(4)
c (Å)	12.968(5)
α (°)	93.71(1)
β (°)	108.02(1)
γ (°)	105.69(1)
V (Å^3)	1157.6(8)
D_{calc} ($g\,cm^{-3}$)	1.416
μ (cm^{-1})	8.57
R_1/wR_2[a]	0.0362/0.1094

[a] $R_1 = \sum||F_o| - |F_c||/\sum|F_o|$; $wR_2 = [\sum w(|F_o| - |F_c|)^2/\sum|F_o|^2]^{1/2}$.

Corp. and Rigaku). Full-matrix least-squares refinements were carried out with anisotropic thermal parameters for all non-hydrogen atoms. All the hydrogen atoms were placed in the calculated positions and fixed. CCDC reference number is CCDC 251440.

3. Results and discussion

3.1. Structure of $[\{Co(NCS)(4\text{-}Phpy)\}_2(\mu\text{-}bpypz)_2]$ (1)

An ORTEP drawing of the structure around the cobalt ions in **1** with the atom numbering scheme is shown in Fig. 1(a). The structure of **1** shows that the desired coordination has been achieved with the cobalt atoms being coordinated to two bpypz to form a dinuclear complex [19]. The dinuclear unit is centrosymmetric, thus, the only one kind of cobalt and ligands exist in the molecule. Each cobalt atom is bound to the four nitrogen atoms of two pyridyl and two pyrazolate moieties in bpypz in the basal plane and two nitrogen atoms of 4-Phpy and NCS^- anion at the axial positions (2.190(4) Å (Co–N(1)), 2.059(3) Å (Co–N(2)), 2.046(3) Å (Co–N(3)), 2.216(4) Å (Co–N(4)), 2.168(4) Å (Co–N(6)), 2.095(4) Å (Co–N(21))) forming a distorted octahedral environment as clearly seen from the top and side views of the molecule. The dihedral angle between pyridyl and phenyl rings in 4-Phpy is 20°, the value of which is smaller than those of $[Ta(NMe_2)Cl_3(4\text{-}Phpy)]$ (40°) [20] and $[Ni(4\text{-}Phpy)_2(DBM)_2]$ (DBM = dibenzoylmethane) (30°) [21]. The efficient packing presumably compensates for

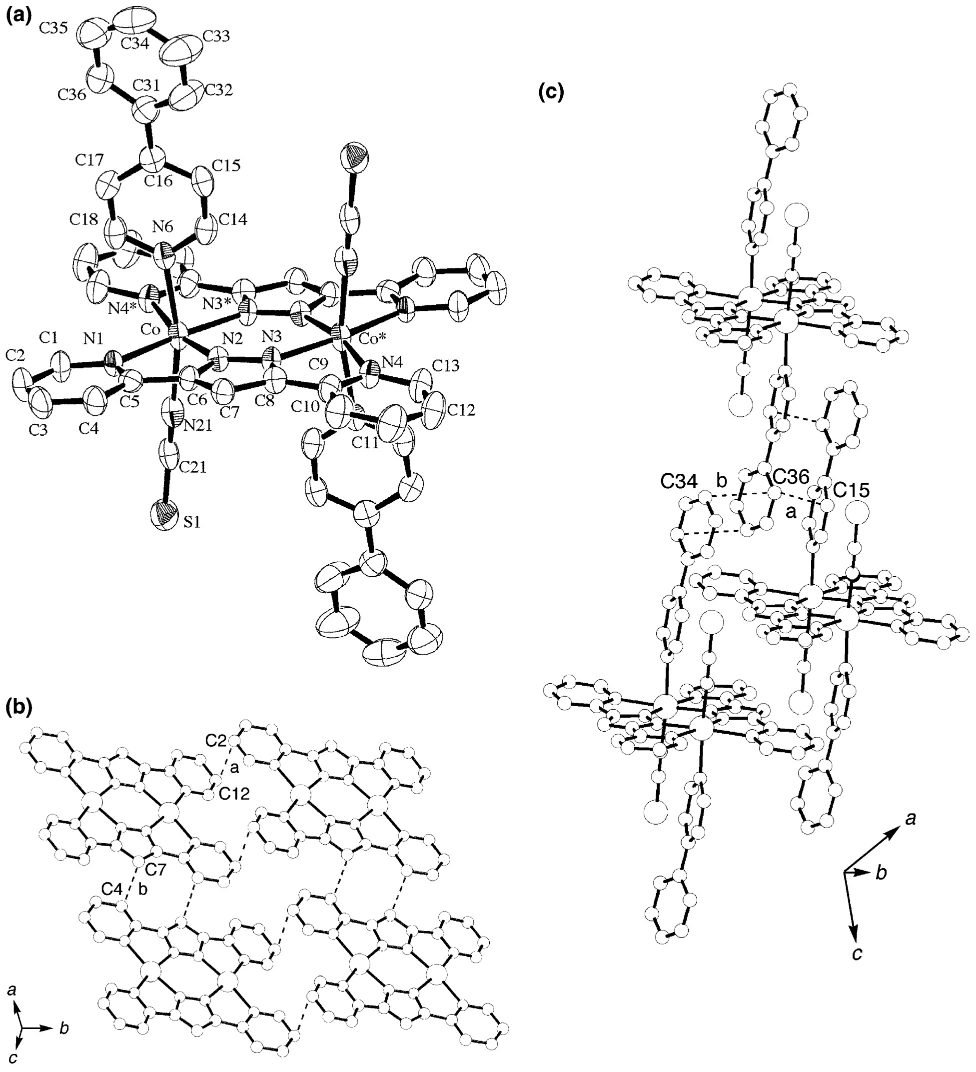

Fig. 1. (a) ORTEP drawing of **1** with atom numbering scheme. Thermal ellipsoids are set at 50% probability and hydrogen atoms have been omitted for clarity. Selected bond distances (Å): Co–N1 2.190(4), Co–N2 2.059(3), Co–N3* 2.046(3), Co–N4* 2.216(4), Co–N6 2.168(4), Co–N21 2.095(4). (b) Emphasizing the π–π stacking interactions between two bpypz ligands of consecutive **1** dimers: *a* (C2–C12) = 3.46 Å, *b* (C4–C7) = 3.42 Å. 4-Phenylpyridine ligands and NCS^- anions have been omitted for clarity. (c) Emphasizing π–π stacking interactions between consecutive 4-phenylpyridine ligands: *a* (C15–C36) = 3.51 Å, *b* (C34–C36) = 3.73 Å.

any unfavorable H—H contact that results in the coordinated 4-Phpy (vide infra). Interestingly, **1** forms a layer by the two types of π–π stacking interactions between the adjacent bpypz ligands of the neighbor dimers (Fig. 1(b)): (1) between pyridyl rings and (2) between pyridyl and pyrazole rings on the adjacent complexes. The layers are connected by additional π–π stacking interactions between adjacent 4-Phpy ligands (Fig. 1(c)) to form a three-dimensional structure.

3.2. Structure of $[\{Fe(NCS)(4\text{-}Phpy)\}_2(\mu\text{-}bpypz)_2]$ (**2**)

Despite many efforts, we did not succeed in growing single crystals of **2** suitable for single crystal X-ray analysis and we used powder diffraction pattern to determine the structure. Fig. 2 shows the diffractograms of compounds **1** and **2** accompanied with the simulated pattern obtained from the crystal structure of **1**. The X-ray diffraction patterns show **1** and **2** to be isomorphous at room temperature, and thus, the dinuclear iron(II) structure is confirmed to be formed.

3.3. Magnetic properties

Fig. 3 shows temperature dependence of the magnetic susceptibilities of the compounds **1** and **2**. The $\chi_M T$ value of **1** in the higher temperature region is about 5.4 emu K mol^{-1}, which is larger than the spin only value for two Co(II) site (3.752 emu K mol^{-1}). This behavior is typical of the high spin Co(II) ion in a distorted octahedral environment, and a large orbital contribution to the magnetic moment should be considered. However, at lower temperature the $\chi_M T$ value dramatically decreases in a manner indicative of intramolecular antiferromagnetic coupling between high spin cobalt(II) ions with a low-lying spin singlet as the ground state. Thus we have attempted to fit the essential feature of the experimental susceptibility by using the simple classical spin approach ($H = -JS_A \cdot S_B$), to give a fitting with $J = -8.78$ cm^{-1} and $g = 2.49$. No spin transition occurs in **1** while J value correlates well to the related high spin cobalt(II) dinuclear complexes reported [22].

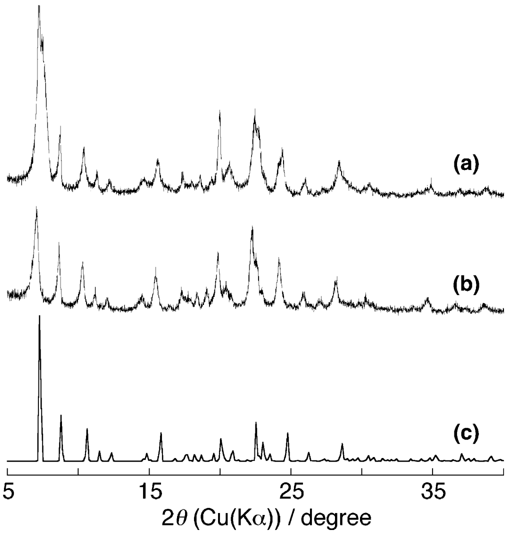

Fig. 2. Powder X-ray diffraction patterns of **1** (a) and **2** (b). (c) shows the simulated pattern obtained from the crystal structure of **1**.

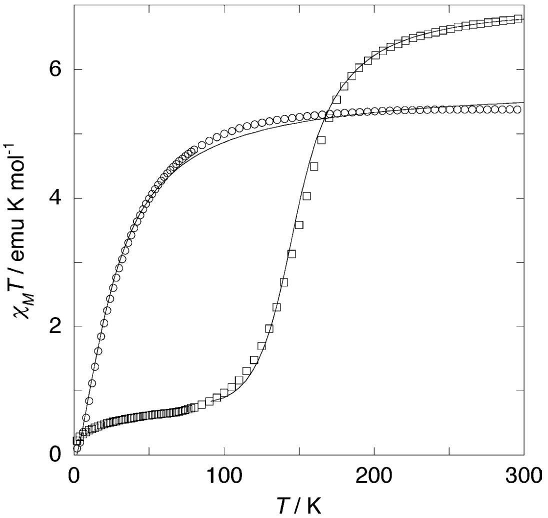

Fig. 3. Temperature dependence of $\chi_M T$ plots for **1** (○) and **2** (□). The solid lines are the fit of the data; see the text for the fitting parameters.

On the other hand, compound **2** shows a spin-crossover phenomenon. The substitution of the metal ion from cobalt to iron leads to the emergence of the spin-crossover. This may be due to the difference in the stability of the low spin phases. The temperature dependence of the $\chi_M T$ value is reversible in both the cooling and warming mode with no hysteresis. The $\chi_M T$ value decreases on lowering the temperature, and then it remains nearly constant at 0.6 emu K mol^{-1}, the value of which corresponds to a mixture of low spin and high spin ions, with the molar fractions 0.17 and 0.83, respectively. Below 40 K, the $\chi_M T$ value slightly decreases, reaching a value of 0.2 emu K mol^{-1} at 2 K. This decrease in the low temperature range may be attributed to the antiferromagnetic coupling of the residual HS sites as seen in the cobalt complex shown above. The spin-crossover temperature T_c (150 K) of complex **2** is higher than that of $[\{Fe(NCS)(py)\}_2(\mu\text{-bpypz})_2]$ (127 K) [23]. The detailed comparison in spin-crossover behavior between these two complexes could be made by the least-squares fitting of the magnetic susceptibility using the regular solution model through Eq. (1) [24].

$$\ln[(1-\gamma_{HS})/\gamma_{HS}] = \Delta H_{HL} + \Gamma(1-2\gamma_{HS})/RT - \Delta S_{HL}/R, \quad (1)$$

where γ_{HS} is the high spin fraction, Γ is an interaction parameter, and ΔH_{HL} and ΔS_{HL} are the enthalpy and entropy change associated with the spin transitions.

The cooperative factor of the spin transition is defined by $C = \Gamma/2RT_c$. A good simulation of the magnetic susceptibility is achieved with $\Delta H_{HL} = 7.18\ \mathrm{kJ\ mol^{-1}}$, $\Delta S_{HL} = 47.9\ \mathrm{J\ K^{-1}\ mol^{-1}}$, $\Gamma = 1.08\ \mathrm{kJ\ mol^{-1}}$ and $C = 0.433$ as indicated by the solid curve in Fig. 3. ΔH_{HL} for **2** is larger than that for [{Fe(NCS)(py)}$_2$(μ-bpypz)$_2$] (5.96 kJ mol^{-1}) whereas ΔS_{HL} is similar to each other ($\Delta S_{HL} = 46.6\ \mathrm{J\ K^{-1}\ mol^{-1}}$ for [{Fe(NCS)(py)}$_2$(μ-bpypz)$_2$]) [23]. Thus, the difference of T_c with the substitution of pyridine moiety for [{Fe(NCS)(X-py)}$_2$(μ-bpypz)$_2$] is attributed in their enthalpy difference. This is similar to the replacement of NCS$^-$ to NCBH$_3{}^-$ moiety for [{Fe(NCX)(py)}$_2$(μ-bpypz)$_2$], but is different from the case for the series of compounds [Fe(PM-L)$_2$(NCX)$_2$] in which ΔS_{HL} is significantly affected by the S/Se substitution of X in NCX$^-$ [24]. Interestingly, the cooperative factor C of **2** is smaller than that of [{Fe(NCS)(py)}$_2$(μ-bpypz)$_2$] indicating that the spin-crossover behavior for **2** is more gradual than that for [{Fe(NCS)(py)}$_2$(μ-bpypz)$_2$] [23]. This may reflect the difference in the crystal packing structure due to the substitution from py to 4-Phpy. Moreover, the spin-crossover in the present dinuclear complex occurs apparently in terms of a single molecular basis rather than by intermolecular interactions as claimed for *cis*-[Fe(NCBH$_3$)$_2$(phen)$_2$] [25]. On the other hand, we have very recently revealed that [{Fe(NCBH$_3$)(4-Phpy)}$_2$(μ-bpypz)$_2$] shows the non-stepwise direct two step spin-crossover through the intermediate magnetic state with the coexistence of [HS–HS] and [LS–LS] dinuclear spin states while the X-ray diffraction patterns show [{Fe(NCX)(4-Phpy)}$_2$(μ-bpypz)$_2$] (X = S, BH$_3$) to be isomorphous at room temperature [17]. Therefore, the intermediate magnetic state can be affected by the subtle change in the molecular structure or the intermolecular interactions such as π–π stacking interactions.

4. Conclusions

We have described the synthesis, structure and magnetic properties of dinuclear complexes using bpypz as the linking ligand. The iron(II) complex exhibits that the spin-crossover occurs with a single HS–HS to LS–LS process, as in the case of the μ-pypz complex [15] while no spin transition occurs in the cobalt(II) complex. The changes in the thermodynamic parameters on the spin-transition of the iron complex are in accordance with those for the corresponding spin-crossover mononuclear iron(II) complexes. The difference of T_c with the substitution of pyridine moiety from py to 4-Phpy for [{Fe(NCS)(X-py)}$_2$(μ-bpypz)$_2$] is attributed in their enthalpy difference. This is similar to the replacement of NCS$^-$ to NCBH$_3{}^-$ moiety for [{Fe(NCX)(py)}$_2$(μ-bpypz)$_2$]. However, the spin transition behavior of the dinuclear complexes cannot be easily understood as exemplified in the comparison between [{Fe(NCX)(4-Phpy)}$_2$(μ-bpypz)$_2$] since it can be affected by the synergy between the inter- and intramolecular interactions. Therefore, further exploration into this series of compounds could give a clue to deeper understanding spin-crossover phenomena in dinuclear complexes.

Acknowledgments

This research was supported by a Grant-in-Aid for Scientific Research (No. 15550050), and by a Grant-in-Aid for Scientific Research on Priority Area (No. 417) from the Ministry of Education, Culture, Sports, Science and Technology, Japan.

References

[1] P. Gütlich, Y. Garcia, H.A. Goodwin, Chem. Soc. Rev. 29 (2000) 419.
[2] J.A. Real, A.B. Gaspar, V. Niel, M.C. Muñoz, Coord. Chem. Rev. 236 (2003) 121.
[3] O. Kahn, C.J. Martinez, Science 279 (1998) 44.
[4] G.J. Halder, C.J. Kepert, B. Moubaraki, K.S. Murray, J.D. Cashion, Science 298 (2002) 1762.
[5] A. Michalowicz, J. Moscovici, B. Ducourant, D. Cracco, O. Kahn, Chem. Mater. 7 (1995) 1833.
[6] Y. Garcia, O. Kahn, L. Rabardel, B. Chansou, L. Salmon, J.P. Tuchagues, Inorg. Chem. 38 (1999) 4663.
[7] P.J. Koningsbruggen, Y. Garcia, O. Kahn, L. Fournès, H. Kooijman, A.L. Spek, J.G. Haasnoot, J. Moscovici, K. Provost, A. Michalowicz, F. Renz, P. Gütlich, Inorg. Chem. 39 (2000) 1891.
[8] S. Hayami, K. Hashiguchi, G. Juhász, M. Ohba, H. Okawa, Y. Maeda, K. Kato, K. Osaka, M. Takata, K. Inoue, Inorg. Chem. 43 (2004) 4124.
[9] A. Real, J. Zarembowitch, O. Kahn, X. Solans, Inorg. Chem. 26 (1987) 2939.
[10] R. Claude, J.-A. Real, J. Zarembowitch, O. Kahn, L. Ouahab, D. Grandjean, K. Boukheddaden, F. Varret, A. Dworkin, Inorg. Chem. 29 (1990) 4442.
[11] J.-A. Real, H. Bolvin, A. Bousseksou, A. Dworkin, O. Kahn, F. Varret, J. Zarembowitch, J. Am. Chem. Soc. 114 (1992) 4650.
[12] J.A. Real, I. Castro, A. Bousseksou, M. Verdaguer, R. Burriel, M. Castro, J. Linares, F. Varret, Inorg. Chem. 36 (1997) 455.
[13] J.-F. Létard, J.A. Real, N. Moliner, A.B. Gaspar, L. Capes, O. Cador, O. Kahn, J. Am. Chem. Soc. 121 (1999) 10630.
[14] V. Ksenofontov, A.B. Gaspar, V. Niel, S. Reiman, J.A. Real, P. Gütlich, Chem. Eur. J. 10 (2004) 1291.
[15] B.A. Leita, B. Moubaraki, K.S. Murray, J.P. Smith, J.D. Cashion, Chem. Commun. (2004) 156.
[16] N. Suemura, M. Ohama, S. Kaizaki, Chem. Commun. (2001) 1538.
[17] K. Nakano, S. Kawata, K. Yoneda, A. Fuyuhiro, T. Yagi, S. Nasu, S. Morimoto, S. Kaizaki, Chem. Commun. (2004) 2892.
[18] G.B. Kauffman, R.A. Alberts, F.L. Harlan, Inorg. Synth. 12 (1970) 251.
[19] M. Munakata, P.L. Wu, M. Yamamoto, T. Kuroda-Sowa, M. Maekawa, S. Kawata, S. Kitagawa, J. Chem. Soc., Dalton Trans. (1995) 4099.
[20] S.W. Schweiger, D.L. Tillison, M.G. Thorn, P.E. Fanwick, I.P. Rothwell, J. Chem. Soc., Dalton Trans. (2001) 2401.

[21] D.V. Soldatov, G.D. Enright, J.A. Ripmeester, Chem. Mater. 14 (2002) 348.
[22] S. Brooker, D.J. Geest, R.J. Kelly, P.G. Plieger, B. Moubaraki, K.S. Murray, G.B. Jameson, J. Chem. Soc., Dalton Trans. (2002) 2080.
[23] K. Nakano, N. Suemura, S. Kawata, A. Fuyuhiro, T. Yagi, S. Nasu, S. Morimoto, S. Kaizaki, Dalton Trans. (2004) 982.
[24] L. Capes, J.-F. Létard, O. Kahn, Chem. Eur. J. 6 (2000) 2246.
[25] K.F. Purcell, M.P. Edwards, Inorg. Chem. 23 (1984) 2620.